C. R. Chimie 21 (2018) 270–276

Contents lists available at ScienceDirect

Comptes Rendus Chimie

www.sciencedirect.com

Full paper/Mémoire

Histamine detection using functionalized porphyrin as electrochemical mediator

Détection de l'histamine par l'utilisation d'une porphyrine fonctionnalisée comme médiateur chimique

Ana-Maria Iordache [a], Rodica Cristescu [b, *], Eugenia Fagadar-Cosma [c], Andrei C. Popescu [b], Anton A. Ciucu [d], Stefan M. Iordache [a], Adriana Balan [a], Cornelia Nichita [a, e], Ioan Stamatin [a], Douglas B. Chrisey [f]

[a] *University of Bucharest, 3 Nano-SAE Research Center, PO Box MG-38, Bucharest-Magurele, Romania*
[b] *National Institute for Lasers, Plasma & Radiation Physics, Lasers Department, PO Box MG-36, Bucharest-Magurele, Romania*
[c] *Institute of Chemistry Timisoara of Romanian Academy, Department of Organic Chemistry, 24 M. Viteazu Avenue, 300223, Timisoara, Romania*
[d] *University of Bucharest, Faculty of Chemistry, Bucharest, Romania*
[e] *National Institute for Chemical-Pharmaceutical Research and Development, 112, Vitan Street, 031299, Bucharest, Romania*
[f] *Department of Physics and Engineering Physics, Tulane University, New Orleans, Louisiana, USA*

ARTICLE INFO

Article history:
Received 3 December 2016
Accepted 29 May 2017
Available online 6 July 2017

Keywords:
Porphyrin
Thin films
Matrix-assisted pulsed laser evaporation
Electrochemical mediator
Histamine electrochemistry

ABSTRACT

This study reports on deposition of asymmetrical substituted *meso*-phenyl porphyrin, 5-(4-carboxyphenyl)-10,15,20-triphenylporphyrin (CPTPP) thin films by matrix-assisted pulsed laser evaporation (MAPLE) on screen-printed electrodes, aiming for histamine detection. Raman spectrometry confirmed that CPTPP chemical structure was preserved in MAPLE-deposited thin films at 200 mJ/cm^2 laser fluence. Atomic force microscopy topography revealed that MAPLE-deposited thin films have a better coverage on the working electrode made of carbon compared to the ones obtained by dropcasting. Cyclic voltammetry demonstrated that CPTPP is an appropriate mediator for histamine detection in trichloroacetic acid solution. We proved that MAPLE serves as a soft technique in fabrication of porphyrin thin films and patterns.

Mots-clés:
Porphyrine
Couches minces
Évaporation laser assistée par matrice
Médiateur électrochimique
Électrochimie de l'histamine

SOMMAIRE

Cet article traite du dépôt de couches minces, par évaporation laser assistée par matrice (MAPLE), de 5-(4-carboxyphényl)-10,15,20-triphénylporphyrine (CPTPP) substituée asymétriquement. Les couches minces ont été déposées sur des électrodes imprimées, avec comme objectif la détection de l'histamine. La spectroscopie Raman a confirmé que la structure chimique de la CPTPP a été préservée dans les couches minces déposées par MAPLE avec une fluence laser de 200 mJ/cm^2. La topographie AFM a révélé une meilleure couverture de l'électrode de carbone par MAPLE par rapport au *dropcast*. La voltamétrie cyclique a démontré que la CPTPP est un médiateur approprié pour la détection de

* Corresponding author.

http://dx.doi.org/10.1016/j.crci.2017.05.008
1631-0748/

l'histamine dans une solution d'acide trichloracétique. On montre que MAPLE est une technique douce pour la fabrication de couches minces et de motifs de porphyrine.

1. Introduction

Histamine is an important biogenic amine present in many foods, vegetables, and fruits. It acts as a chemical messenger in biological systems [1–3]. When food is not processed and packed in hygienic conditions, the amounts of histamine and all biogenic amines can increase to toxic levels. The meat freshness is related to the level of biogenic amines (histamine, cadaverine, and putrescine to name few [4]). For histamine, the caution level is 50 ppm, whereas the maximum accepted levels range from 200 ppm (in EU) to 500 ppm (USA), respectively [5]. Such a low level of detection requires advanced functional materials with high sensibility/selectivity in chemosensor science. Traditionally, high performance liquid *chromatography* (HPLC) mass spectrometry is used to analyze the biogenic amines with precolumn or postcolumn derivatization [1,6,7]. The electrochemical methods, inexpensive and less time-consuming in analysis, still have to overcome the high oxidation potential and all polyamines that are considered electroinactive in aqueous solutions [8]. For instance, the histamine has the oxidation potential ∽1.2 V versus standard calomel electrode in 0.1 M phosphate-buffered solution (pH = 7) at a glassy carbon or boron-doped diamond electrode [9]. These values are close to the water oxidation, with respect to the carbon electrode oxidation that induces a high background current. There are three approaches in designing electrochemical sensors for biogenic amine detection: (1) mediator-less electrode with large window potential such as boron-doped diamond films or oxides with transfer of oxygen atoms from H_2O to the analyte oxidation [6,10]; (2) enzyme-modified electrode (amino-oxidases or horseradish peroxidase) [11,12] where the oxidation potential reduces down to +700 mV versus Ag/AgCl; and (3) chemically modified electrode with different sensitive layers, nanoparticles, and so forth [13,14]. The chemically modified electrodes with porphyrins and metalloporphyrins have opened a new approach in sensing of biogenic amines taking into account their ability in molecular recognition for different analytes [15–18]: (1) Porphyrins have a large window potential on average 2.2 V between oxidation and reduction potentials [19,20]. (2) The oxidation potential is close to the oxidation potentials of the biogenic amines, favorable to design a porphyrin-based screen-printed electrode (SPE). (3) They could be bonded to the electrode (carbon paste, glassy carbon, carbon nanopowders, etc.) via carboxyl or hydroxyl groups during surface treatment [21,22]. (4) Porphyrins are known as building blocks for a large class of biomolecules, biocatalysts with extensive applications in life processes, and in sensing. For example, chlorophyll fluorescence is used for monitoring CO_2 uptake by earth vegetation [23] or new optoelectronic devices in hybrid combinations with other biomolecules [24,25]. (5) Low solubility in water to allow for the use of acidic or basic water solutions as electrolyte with different biomolecules. (6) The dications of free base porphyrins (generated in acidic electrolyte solutions) have a high affinity for the electron-donating molecules reducing their oxidation potentials or amplifying the electron transfer to the electrode surface [15].

There are few porphyrin-related reports for biogenic amine sensing [26]; to date, there has been no optimized couple, chemically modified electrode–appropriate electrolyte, that could initiate the electrochemical oxidation of biogenic amines in a potential window less than 1 V. In this respect, we propose to explore the histamine sensing using a novel asymmetrical substituted *meso*-phenyl porphyrin, namely, 5-(4-carboxyphenyl)-10,15,20-triphenylporphyrin (CPTPP) thin films deposited on an SPE by matrix-assisted pulsed laser evaporation (MAPLE) [27,28]. MAPLE technique has been enabled to transfer complex molecules onto a substrate at a specific laser fluence, preserving the conformational and molecular structure, thus maintaining the intrinsic properties [29] including, in this case, the sensing capability [30–32]. The electrolyte consists of aqueous trichloroacetic acid (TCA) solution. TCA is used in standard HPLC methods for derivatization of biogenic amines, acting as an electron acceptor. The molecular complex TCA–histamine has a high electronegativity, favorable for both the improved electron transfer and CPTPP oxidation. This work shows that the histamine is not directly electro-oxidized, rather the CPTPP oxidation is improved by TCA–histamine complex.

2. Experimental section

2.1. Materials and methods

Sensitive layer consists of asymmetrical substituted *meso*-phenyl porphyrin, CPTPP, synthesized and characterized similar to previously reported [33–35]. In text, H_2TPP–*p*-COOH (Fig. 2) will be used also for discussions in Section 3.3. H_2TPP– refers to the free base tetraphenylporphyrin macrocycle, whereas –*p*-COOH represents the *p*-carboxyphenyl as the only functional substituted group on *meso* position of the porphyrin periphery.

The SPE (SPE-110, DropSense) contains three electrodes: (1) a working electrode (WE), which is a carbon disc with 4 mm diameter; (2) a counter electrode ring at 1 mm distance from WE; and (3) a Ag ring pseudoreference electrode. SPE-110 is convenient for working with maximum 50 μL volume (Fig. 3 inset).

For comparison, two SPEs are fabricated: (1) SPE with CPTPP dropcasted over WE from a solution of 1% CPTPP in

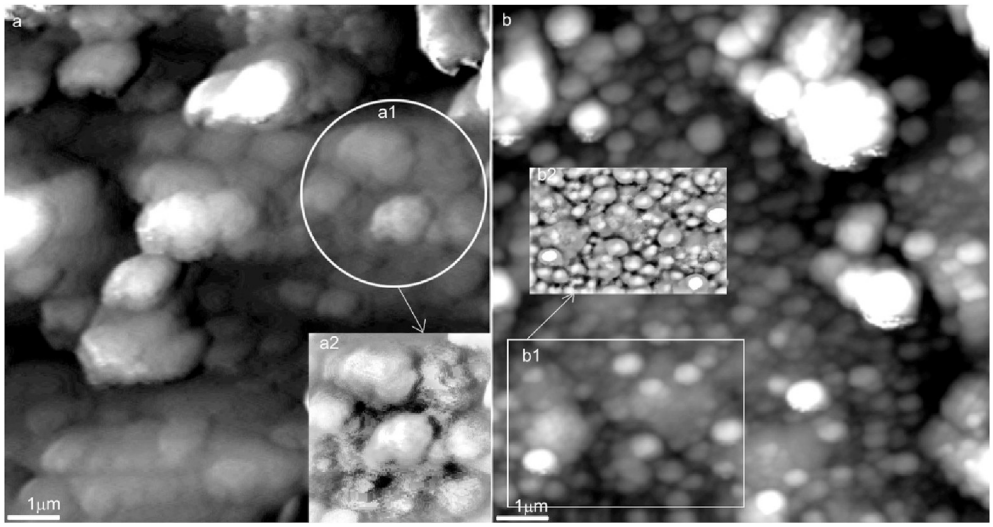

Fig. 1. AFM topography: (a) dropcasted porphyrin layer (SPE-D) and (b) MAPLE-deposited porphyrin thin films over a carbon working electrode area at 200 mJ/cm^2 laser fluence, 20,000 pulses (SPE-M).

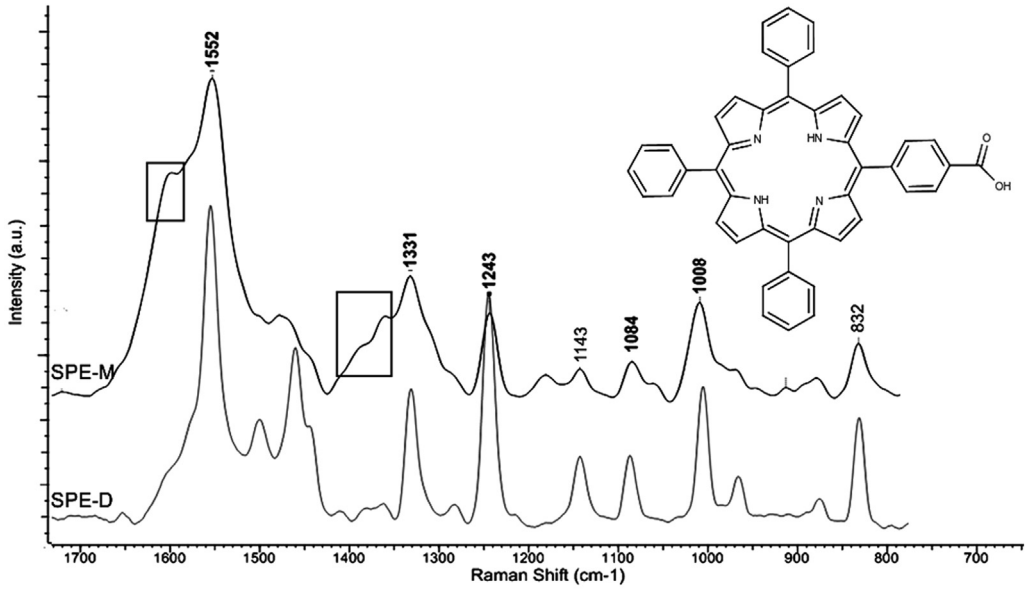

Fig. 2. Typical Raman spectra. Porphyrin deposited by dropcasting (SPE-D) and by MAPLE (SPE-M). Rectangles—contribution from carbon electrode (G or D bands, respectively). In inset the CPTPP molecular structure is given.

chloroform with drying at 50 °C overnight in desiccator (SPE-D), and (2) SPE with CPTPP deposited by MAPLE technique (SPE-M) as described subsequently.

All chemicals were used as received. Histamine, TCA, and phosphate-buffered saline solutions (pH = 7.4) of analytical grade were purchased from Sigma–Aldrich. Electrolyte consisted of 0.02 M TCA in HPLC water. Stock solutions for tests with concentrations within the range of 0.7–100 ppm histamine in 0.02 M TCA were prepared, flushed with nitrogen, and stored in nitrogen atmosphere to remove dissolved oxygen in water. For each electrochemical analysis, 40 μL of stock solutions with histamine in 0.02 M TCA were dropped over SPE.

2.2. MAPLE experimental conditions

For MAPLE depositions, 0.2 g CPTPP was homogenously suspended in a 20 mL chloroform organic solvent by ultrasonically stirring. Then 3.5 mL of obtained solution was poured in a precooled target holder. After that, the holder was immersed in nitrogen liquid (LN_2) for 30 min, and the solution was frozen at 173 K. This was further used as a solid target in the deposition chamber where a cooler supplied with LN_2 flow kept it frozen during the multipulse irradiation and evaporation.

MAPLE depositions of CPTPP thin films were conducted using a KrF* ($\lambda = 248$ nm, $\tau_{FWHM} = 25$ ns, and pulse

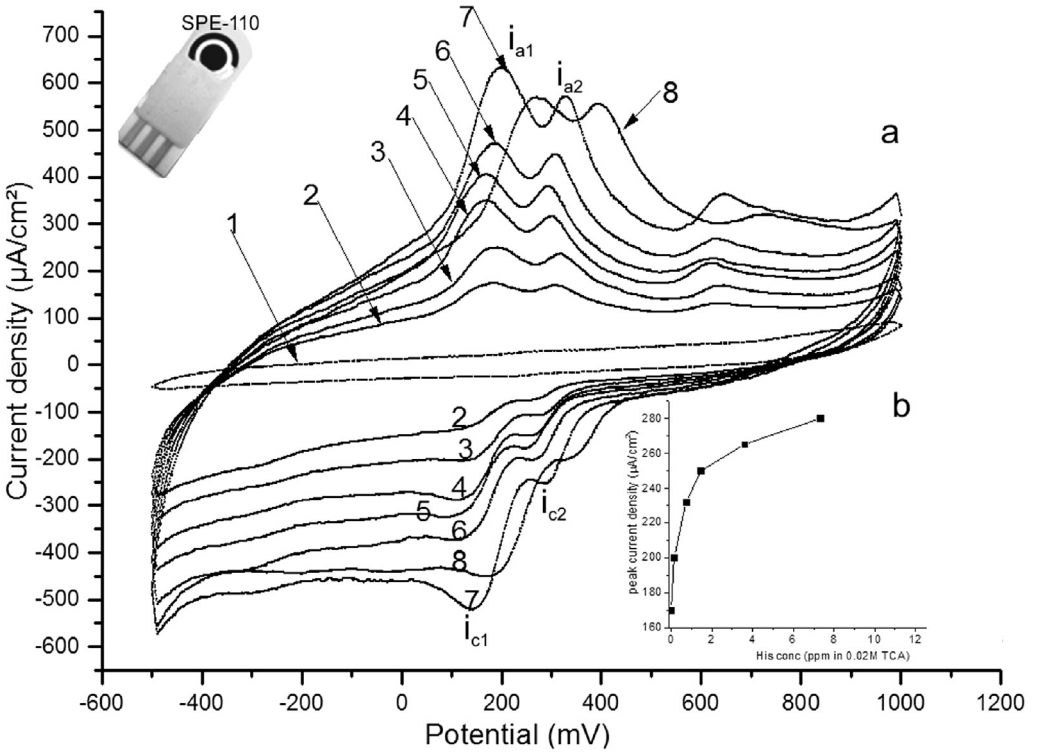

Fig. 3. a) Cyclic voltammetry on SPE-110 (1), SPE-M without TCA for 15 ppm histamine in buffer solution (2), and SPE-M in 0.02 M TCA for 0.15 ppm histamine (3), 0.73 ppm histamine (4), 1.5 ppm histamine (5), 3.7 ppm histamine (6), 7.3 ppm histamine (7), and 15 ppm histamine (8). (Curves 3, 4, 5, 6, 7, 8 are multiplied with by factors 1.25, 1.5, 1.75, 2, 2.25, 2.25.) i_a and i_c are current density for anodic and cathodic waves, respectively. (b) Example of calibration curve showing the dependence between the current density of first oxidation peak (i_{a1}) and histamine concentration (ppm). Inset: SPE-110 (DropSense).

repetition rate = 10 Hz) excimer laser source that was operated at a fluence of 200 mJ/cm^2 and for 10,000–20,000 subsequent laser pulses. The laser spot area was set at 10.2 mm^2. The target was rotated at a rate of 0.4 Hz during deposition to avoid heating and damage by the pulsed laser beam. During MAPLE deposition, the laser beam scanned the entire target surface at an angle of 45°. All depositions were conducted in a vacuum reaction chamber with a background pressure of 30–40 Pa and substrate-to-target distance of 4 cm. Thin films were deposited onto double-side polished Si ⟨100⟩ substrates for atomic force microscopy (AFM) and Raman spectrometry investigations, and SPE-M substrates for electrochemical analysis. For comparison data, a control set of films (SPE-D) was prepared by dropcasting on the same Si ⟨100⟩ substrates. Before MAPLE deposition, SPE-M WE area was cleaned by immersion in an Elma Transsonic T 310 ultrasonic bath (Elma GmbH & Co. KG, Singen, Germany), filled with ethanol, and then dried in air under UV exposure from a VL-115 UV lamp (VilberLourmat, Marne-la-Vallee Cedex, France). For the optimum deposition rate, the laser fluence was adjusted at the value of 200 mJ/cm^2. Over this threshold, CPTPP loses its structure integrity, whereas for a value less than 150 mJ/cm^2 the deposition rate is very low.

2.3. Material characterization

An AFM SPM (NTegra Prima, NT-MDT) platform was used in semi-contact mode. Thin film thickness was recorded using a Stylus Profiler XP-2 system (Ambios) with a 0.1 nm vertical resolution, an optical deflection height-measurement sensor and stylus with a 2.5 μm radius and 0.1 mg force. Raman spectrometry spectra of thin films were collected using a Jasco NRS 3100 with dual laser beams, 532 nm wavelength. Electrochemical analysis was performed using a Voltalab 40 system (Radiometer Analytical) adapted for SPEs to perform linear sweep voltammetry and cyclic voltammetry at different scan rates.

3. Results and discussions

3.1. AFM topography

AFM micrographs of CPTPP thin films deposited both using MAPLE technique (SPE-M) at the 200 mJ/cm^2 laser fluence and simple dropcast method (SPE-D) are shown in Fig. 1. Films deposited by dropcast (SPE-D, Fig. 1a) are quite different in both morphology and topography in comparison with those deposited by MAPLE (SPE-M) (Fig. 1b). Dropcast-deposited films are made of aggregates randomly distributed on the electrode surface, some of them being stacked. Their dimensions range from 200 to 300 nm up to 1.2 μm (Fig. 1a, insets a1 and a2). CPTPP porphyrin thin films deposited on SPE-M show small spherulitic particles evenly spread across the electrode surface (Fig. 1b). Their dimensions range from 100 to 200 nm. When the number of pulse increases over 20,000, the aggregation of particles

is noticed. In Fig. 1b (inset b2 shows a detail of inset b1), a uniform distribution of spherulitic porphyrins covering the electrode surface can be observed. Root mean square (RMS) average roughness reaches ∽70 nm. According to our measurements, the films thickness was 300 ± 30 nm.

The laser fluence, concentration of porphyrin in the frozen target, and the number of pulses are the parameters that significantly influence the films morphology [36,37]. Laser fluence dominates the preservation of both structure and conformation of the molecules evaporated and then transferred to substrate. Optimum laser fluence established in this work was ∽200 mJ/cm^2. The increase in either solute concentration and/or number of pulses applied for the deposition of one film cause the molecule aggregation in spherulitic shapes and their further agglomeration, respectively.

3.2. Raman spectrometry

Typical Raman spectra reveal the level of degradation/preservation of the CPTPP molecular structure and composition by comparison between dropcast-obtained coatings (SPE-D) and MAPLE-deposited thin films (SPE-M). The characteristic bands of CPTPP were identified both in the dropcast-obtained coatings (SPE-D) and MAPLE-deposited thin films (SPE-M), and the band assignments are being summarized in Table 1.

Both dropcast-obtained coatings (SPE-D) and MAPLE-deposited thin films (SPE-M) have similar Raman bands for laser fluences up to 200 mJ/cm^2 (Fig. 2).

The peaks of MAPLE-deposited-films (SPE-M) are broader, with low intensity shoulders, suggesting an overtone of several vibration modes. In the case of SPE-D films, the Raman spectra have well-defined peaks, with a narrow Gaussian distribution and rare shoulders. This aspect corresponds to a physical aggregation of the particles [50], without chemical interaction (in agreement with the AFM micrograph, Fig. 1a) that is also observed in Ref. [38]. In this case, the vibrational modes for C_α–C_m and C_α–N have either upshifts or downshifts. This strongly depends on both the shortening of single bonds and lengthening of double bonds and may be related to a loss of planarity of the porphyrin cycle. This effect can be observed in the MAPLE film spectra (SPE-M), in which the bands centered at 1552, 1477, and 1331 cm^{-1} are slightly shifted in comparison to the SPE-D films. When comparing the typical porphyrin skeleton vibration bands centered at 1552, 1243, and 1084 cm^{-1}, no shift can be observed in the both films. However, two low intensity bands centered at 1180 and 912 cm^{-1} are observed in the MAPLE spectra (SPE-M). These bands correspond to the pyrrole breathing mode [39], and are assigned to the deformation of the C–N–H bond angles. The carbon substrate bands (assigned to G and D bands, respectively) are indexed in the rectangle areas on SPE-M spectrum.

Table 1
Band assignments of the Raman spectra of CPTPP.

Band (cm^{-1})	Vibration mode assigned	Reference
1552	ν_{asymm} (C_α–C_m) porphyrin ring skeleton + symmetric stretching motion of four C_β–C_β bonds	[41–43]
1477	ν_{symm}(C_β–C_β, C_α–C_m) phenyl ring	[44]
1331	ν_{symm} ($C_{pyrrole}$) pyrrole skeleton, in-phase and out-of-phase symmetric half-ring motion of pyrrole ring	[32,45]
1243	δ_{sym}(C_β–H) pyrrole skeleton	[32,46]
1180	ν_{asymm} (C_α–N) + N–H bend	[32,33]
1142	ν_{symm} (C_α–H) pyrrole skeleton	[30,32]
1084	ν_{symm} (C_β–H)	[30,33]
1008	ν_{breath} (pyrrole) + ν_{symm} phenyl skeleton + ν (C_α–C_β) + ν (N–C_α) + porphyrin skeleton	[22,31,43,47,48]
912	ν_{asymm} (C_α–N) + N–H bend	[22,33]
878	ν_{symm} (phenyl)	[33]
831	δ_{sym}pyrrole skeleton and ν (pyrolic deformation)	[32,49]

3.3. Electrochemical analysis—cyclic voltammetry

The cyclic voltammetry method gives information related to the redox reactions for one analyte at the interface electrode mediator in an appropriate electrolyte support. Histamine (the analyte used in our studies) has a high oxidation potential (∽1.2 V [9]) and TCA an electroreduction potential down to ~−700 mV [40]. For any aqueous solution, when a WE-based carbon is used, the maximum potential window cannot be higher than 1.23 V; otherwise the electrolysis is taking place. Therefore, the cyclic voltammograms are recorded within the potential window −400 to 1000 mV. The cyclic voltammograms recorded on SPE-110 at different concentrations (up to 15 ppm) for both histamine–buffer solutions and histamine–0.02 M TCA have no electrochemical activity (Fig. 3a, curve 1); even for high concentrations, there is no electrochemical response. When CPTPP is immobilized on SPE (SPE-M) and cyclic voltammograms are recorded for histamine at high concentration (15 ppm in buffer solution, Fig. 3, curve 2), several very weak oxidation peaks are identified around of 180, 300, and 640 mV. This seems to be interesting because the earlier studies on carboxyphenyl-H_2TPP electroactivity in organic solvents (such as CH_2Cl_2) have shown weak oxidation peaks at ∽600 and ∽840 mV, respectively. This behavior depends on the scanning rate [41] and is assigned to the π-dication H_2TPP macrocycle. The only assumption is that the histamine can react with the COOH group from CPTPP by changing the oxidation potentials to the lower value for π-dication H_2TPP macrocycle. Previous studies have proved that the histamine can be protonated/deprotonated in –COOH/acetate aqueous media (using acetic acid as reference; the acid acetic acid dissociation constant (pK_a) is ∽4.76) [51].

By comparison, the carboxyphenyl group from CPTPP has an appropriate pK_a similar to the one of the benzoic acid (pK_a ∽4.2). This group is expected to form a CPTPP–histamine complex where the dications of free base porphyrins have lower oxidation potentials. The very weak response in current density, even for high concentration (Fig. 3a, curve 2), indicates that there are several potential barriers and steric effects that have direct access to the –COOH by histamine.

In the case of a strong acid, such as TCA (pK_a ∽0.66), the histamine is readily derivatized in histamine-

trichloroacetate (by the same protonation mechanism [51]), used as standard methods in HPLC [1,6,7]. As previously demonstrated [51], the histamine has three protonation sites. Therefore, the histamine–TCA molecular complex becomes more effective in generation of $-H_2TPP$ dications within the acidic electrolyte solutions at lower oxidation potentials and thus improving the electron transfer to the electrode surface [15]. This happens when CPTPP is immobilized on SPE, the cyclic voltammograms show several oxidation peaks assigned to H_2TPP macrocycle oxidation (the first two peaks at ∽180 and ∽300 mV, respectively, on the anodic waves) and a third oxidation peak at ∽640 mV (Fig. 3a, curves 3–8). Replacing the electrolyte with an electron acceptor (TCA) in the presence of histamine, the oxidation of the H_2TPP macrocycle is improved with well-defined two reversible redox peaks assigned to the reactions:

$$H_2TPP{-}p-COOH \rightarrow (H_2TPP)^{\cdot+}{-}p-COOH, \quad \text{first oxidation state } (\sim 180\ \text{mV}) \tag{1}$$

$$(H_2TPP)^{\cdot+}{-}p-COOH \rightarrow (H_2TPP)^{2+}{-}p-COOH, \quad \text{second oxidation state } (\sim 300\ \text{mV}) \tag{2}$$

These electropositive macrocycles, $(H_2TPP)^+$, could generate intermolecular hydrogen bonds from vicinal $-p$-COOH and might be self-reduced, but unexpectedly, due to porphyrin versatility are irreversibly oxidized at ∽640 mV.

On the other hand, when the histamine is added into the TCA electrolyte, the current density for both the first oxidation peak (i_a) and reduction (i_c), respectively, increase with a ratio $(i_c/i_a)_1 \approx 1$, which is a quasi-reversible process for the first oxidoreduction state. Both oxidation peaks reach to maximum when the histamine concentration is 7–8 ppm (Fig. 3a, curves 2–7). The current density for the second oxidation peak increases with the histamine concentration, whereas $(i_c/i_a)_2 < 1$, signifying a quasi-reversible reaction with intermolecular transfer. The last oxidation peak (∽640 mV) has a similar behavior to that of the first oxidation peak. When the histamine concentration is >8 ppm in 0.02 M TCA, the oxidation peaks shift to higher potentials with ~100–120 mV; the oxidation peaks on the anodic wave decrease; the reduction peak on the cathodic wave remain approximately constant (Fig. 3a, curve 8).

These findings lead to the several assumptions: (1) TCA could be an appropriate electrolyte for a specific class of water insoluble porphyrins (electron acceptor). (2) TCA –histamine complex has a high electronegativity, being favorable to the first electro-oxidation state in CPTPP, when the current density increases with the histamine concentration. Earlier studies have shown the TCA ability to extract histamine from tissues due to its participation in a loose complex containing histamine [44]. It is supposed the formation of molecular complexes between these substances, one acting as an electron donor and the TCA acting as an electron acceptor. This molecular complex has a high electronegativity because of the three chlorine atoms from TCA and histamine with polyprotic behavior containing three protonation sites [15], and the molecular structure would be similar to those formed between aromatic compounds and various electron acceptors [52,53]. On the other hand, almost all porphyrins could be stepwise electro-oxidized or electro-reduced by two electrons at the aromatic π-ring system to give either π-cations or dications and π-anions or dianions, respectively [19]. The window potential (here the potential energy difference between the highest occupied molecular orbital (HOMO) and the lowest unoccupied molecular orbital (LUMO), referred to as the HOMO–LUMO band gap) in the presence of the molecular complexes with high electronegativity is expected to be reduced and the electrochemical response to be dependent of concentrations. (3) The first oxidation peak is electrochemically and chemically reversible, respectively, $(i_c/i_a)_1 \approx 1$. The second peak is electrochemically reversible but chemically irreversible, $(i_c/i_a)_2 < 1.4$. Over the histamine concentration of 7–8 ppm, the oxidation peaks are overlapping and the reduction peaks reach to a plateau. This could be assigned to a maximum concentration of molecular complex histamine–TCA. (5) When the TCA solutions change from 0.02 to 0.04 and 0.06 M, respectively, the histamine detection could reach concentration of 30 and 60 ppm, respectively. Unfortunately, a high TCA concentration deteriorates the plastic protective cover and needs an improvement design for SPE-110.

Fig. 3b exhibits an example of a calibration curve showing the dependence between the current density for the first oxidation peak and the histamine concentration. As visible from Fig. 3b, the detection limit of the sensor for histamine in 0.02 M TCA is within the range of 0–8 ppm.

4. Conclusions

The asymmetrical substituted *meso*-phenyl porphyrin, CPTPP was investigated as a sensitive layer in an electrochemical sensor for the trace detection of histamine, a chemical compound associated with the freshness of meat products. The sensitive layer was deposited onto the carbon working area of SPE-110 using MAPLE technique at 200 mJ/cm^2 laser fluence with well preservation of both the structure and functionality of porphyrin confirmed by AFM and Raman spectrometry. The cyclic voltammetry performed on SPE-M TCA solution opens a new approach to exploit the porphyrin properties as mediator. More specific, the porphyrins with –COOH functional groups, such as CPTPP, open a new way for detection of various amino compounds of large interest in food safety and biochemistry fields. The results show several directions that need to be further investigated: the design of novel porphyrins with more than one –COOH functional group and identification of mechanisms that drive the interaction between –COOH and amino compounds. These directions could give insights into the novel design of chemosensors with porphyrin mediators for analyte concentrations ranging from picomole to micromole in an aqueous noncorrosive electrolyte.

In this study it is shown that the oxidation peaks depend on the concentration of histamine; because of its electronegative effect, TCA influences the oxidation of the H_2TPP macrocycle at lower potentials; the histamine–TCA compound increases the number of H_2TPP mono- and di-cations that are reflected in the current densities for each oxidation–reduction peak; and the saturation effect of

current densities for each oxidation peak can be associated with the maximum number of generated H_2TPP mono-and di-cations (i.e. to the quantity of CPTPP deposited by MAPLE). The detection limit of the sensor for histamine is within the range of 0–8 ppm. The data suggest that CPTPP thin films can be used for the electrochemical detection of histamine for a disposable sensor useful for food quality control.

Acknowledgments

The work was supported by grants from the Romanian National Authority for Scientific Research, CNCS-UEFISCDI: PN-II-PT-PCCA-2013-4-1268 (142/2014), PN-II-PCCA-210/2014, PN-II-ID-PCE-2011-3-0888 (209/2011), and PN-II-RU-TE-2012-3-0379 (16/2013). E.F.-C. is acknowledging Romanian Academy for Programme 3 of ICT.

References

[1] V. Frattini, C.J. Lionetti, J. Chromatogr. A 809 (1998) 241–245.
[2] B.P. Jackson, S.M. Dietz, R.M. Wightman, Anal. Chem. 67 (1995) 1115–1120.
[3] K. Pihel, S. Hsieh, J.W. Jorgenson, R.M. Wightman, Anal. Chem. 67 (1995) 4514–4521.
[4] S.M.H. Silla, Int. J. Food Microbiol. 29 (1996) 213–231.
[5] T. Sato, T. Horiuchi, I. Nishimura, Anal. Biochem. 346 (2005) 320–326.
[6] A. Onal, Food Chem. 103 (2007) 1475–1486.
[7] S. Moret, R.J. Bortolomeazzi, J. Chromatogr. 591 (1992) 175–180.
[8] R.N. Adams (Ed.), Electrochemistry at Solid Electrodes (Monographs in Electroanalytical Chemistry and Electrochemistry, Marcel Dekker Inc., New York, 1969.
[9] B.V. Sarada, T.N. Rao, D.A. Tryk, A. Fujishima, Anal. Chem. 72 (2000) 1632–1638.
[10] L. He, J.R. Anderson, H.F. Franzen, D.C. Johnson, Chem. Mater. 9 (1997) 715–722.
[11] S. Tombelli, M. Mascini, Anal. Chim. Acta 358 (3) (1998) 277–284.
[12] R. Draiscia, G. Volpea, L. Lucentinia, A. Ceciliaa, R. Federicob, G. Palleschi, Food Chem. 62 (2) (1998) 225–232.
[13] M.B. Gumpua, N. Nesakumara, S. Sethuramana, U.M. Krishnana, J. Bosco, B. Rayappan, Sens. Actuators, B 199 (2014) 330–338.
[14] J.H.T. Luong, S. Hrapovic, D. Wang, Electroanalysis 17 (2005) 47–53.
[15] M. Cuartero, C.G. Amorim, A.N. Araújo, J.A. Ortuno, M.C.B.S.M. Montenegro, Anal. Chim. Acta 787 (2013) 57–63.
[16] X. Lu, Y. Quan, Z. Xue, B. Wu, H. Qi, D. Liu, Colloids Surf., B 88 (2011) 396–401.
[17] A. Wong, M.D.P.T. Sotomayor, Sens. Actuators, B 181 (2013) 332–339.
[18] V.K. Gupta, A.K. Jain, Z. Ishtaiwi, H. Lang, G. Maheshwari, Talanta 73 (2007) 803–811.
[19] K.M. Kadish, E.V. Caemelbecke, J. Solid State Electrochem 7 (2003) 254–258.
[20] S. Ishihara, J. Labuta, W. Van Rossom, D. Ishikawa, K. Minami, J.P. Hillab, K. Ariga, Phys. Chem. Chem. Phys. 16 (2014) 9713–9746.
[21] K. Ravichandran, R.P. Baldwin, J. Electroanal. Chem. 126 (1981) 293–300.
[22] E. Fagadar-Cosma, I. Sebarchievici, I. Lascu, I. Creanga, A. Palade, M. Birdeanu, B. Taranu, G. Fagadar-Cosma, J. Alloys Compd. 686 (2016) 896–904.
[23] C. Frankenberg, C. O'Dell, J. Berry, L. Guanter, J. Joiner, P. Köhler, R. Pollock, T.E. Taylor, Remote Sens. Environ. 147 (2014) 1–12.
[24] M.E. Barbinta Patrascu, L. Ţugulea, I. Lacatusu, A. Meghea, Mol. Cryst. Liq. Cryst. 522 (2010) 148–158.
[25] T. Stefanescu, C. Manole, C. Parvu, M.E. Barbinta Patrascu, L. Tugulea, OAM-RC 4 (1) (2010) 33–38.
[26] M.G. Manera, E. Ferreiro-Vila, J.M. García-Martín, A. Cebollada, A. García-Martín, G. Giancane, L. Valli, R. Rella, Sens. Actuators, B 182 (2013) 232–238.
[27] R. A. McGill and D. B. Chrisey, Method of producing a film coating by matrix assisted pulsed laser deposition. U.S. Patent No. 6,025,036, 2000.
[28] D.B. Chrisey, R.A. McGill, J.S. Horwitz, A. Pique, B.R. Ringeisen, D.M. Bubb, P.K. Wu, Chem. Rev. 103 (2003) 553–576.
[29] R. Frycek, F. Vyslouzil, V. Myslik, M. Vrnata, D. Kopecky, O. Ekrt, P. Fitl, M. Jelinek, T. Kocourek, R. Sipula, Sens. Actuators, B 125 (2007) 189–194.
[30] R. Cristescu, C. Popescu, A.C. Popescu, I.N. Mihailescu, A.A. Ciucu, A. Andronie, S. Iordache, I. Stamatin, E. Fagadar-Cosma, D.B. Chrisey, Mater. Sci. Eng., B 169 (2010) 106–110.
[31] R. Cristescu, C. Popescu, A.C. Popescu, S. Grigorescu, I.N. Mihailescu, A.A. Ciucu, S. Iordache, A. Andronie, I. Stamatin, E. Fagadar-Cosma, D.B. Chrisey, Appl. Surf. Sci. 257 (2011) 5293–5297.
[32] S. Iordache, R. Cristescu, A.C. Popescu, C.E. Popescu, G. Dorcioman, I.N. Mihailescu, A.A. Ciucu, A. Balan, I. Stamatin, E. Fagadar-Cosma, D.B. Chrisey, Appl. Surf. Sci. 278 (2013) 207–210.
[33] D. Vlascici, E. Fagadar-Cosma, I. Popa, V. Chiriac, M. Gil-Agusti, Sensors 12 (2012) 8193–8203.
[34] E. Fagadar-Cosma, G. Fagadar-Cosma, M. Vasile, C. Enache, Curr. Org. Chem. 16 (2012) 931–941.
[35] E. Fagadar-Cosma, L. Cseh, V. Badea, G. Fagadar-Cosma, D. Vlascici, Comb. Chem. High T. Scr. 10 (2007) 466–472.
[36] M. Jelinek, T. Kocourek, J. Remsa, R. Cristescu, I.N. Mihailescu, D.B. Chrisey, Las. Phys. 17 (2007) 66–70.
[37] A.P. Caricato, in: M. Castillejo, P.M. Ossi, L. Zhigilei (Eds.), Lasers in Materials Science, Springer Science & Business Media, Heidelberg, New York, Dordrecht, London, 2014, p. 295.
[38] X. Guo, J. Mol. Struct. 892 (2008) 378–383.
[39] X. Guo, B. Guo, T. Shi, Inorg. Chim. Acta 363 (2010) 317–323.
[40] M. Jina, H. Maa, Russ. J. Electrochem. 49 (11) (2013) 1081–1085.
[41] R.F. Shago, Syntheses, Electrochemistry and Spectroscopic Studies of Metallocene-containing Porphyrin Complexes with Biomedical Applications, PhD thesis, University of Free State, South Africa, 2010, p. 110.
[42] X.-Y. Li, R.S. Czernuszewicz, J.R. Kincaid, Y.O. Su, T.G. Spiro, J. Phys. Chem. 94 (1990) 31–47.
[43] Y.-H. Zhang, W. Zhao, P. Jiang, L.-J. Zhang, T. Zhang, J. Wang, Spectrochim. Acta, Part A 75 (2010) 880–890.
[44] B. Robinson, D.M. Shepherd, J. Pharmacol. Pharm. 13 (1) (1961) 374–377.
[45] Y.-H. Zhang, W.-J. Ruan, Z.-Y. Li, Y. Wu, J.-Y. Zheng, Chem. Phys. 315 (2005) 201–213.
[46] G.T. Webster, L. Tilley, S. Deed, D. McNaughton, B.R. Wood, FEBS Lett. 582 (7) (2008) 1087–1092.
[47] T.S. Rush III, P.M. Kozlowski, C.A. Piffat, R.M. Kumble, Z. Zgierski, T.G. Spiro, J. Phys. Chem. B 104 (2000) 5020–5034.
[48] H. van der Salm, S.J. Lind, M.J. Griffith, P. Wagner, G.G. Wallace, D.L. Officer, K.C. Gordon, J. Phys. Chem. C 119 (39) (2015) 22379–22391.
[49] R. Franco, S. Al-Karadaghi, G.C. Ferreira, J. Porphyr. Phthalocyanines 15 (5) (2011) 357–363.
[50] R. Franco, J.L. Jacobsen, H. Wang, Z. Wang, K. Istvan, N.E. Schore, Y. Song, C.J. Medforth, J.A. Shelnutt, Phys. Chem. Chem. Phys. 12 (2010) 4072–4077.
[51] H.A. De Abreu, W.B. De Almeida, H.A. Duarte, Chem. Phys. Lett. 383 (2004) 47–52.
[52] S.P. McGlynn, Chem. Rev. 58 (1958) 1113–1156.
[53] D. Wang, X. Cheng, Y. Shi, E. Sun, X. Tang, C. Zhuang, T. Shi, Solid State Sci. 11 (2009) 195–199.